Journal of Environmental Chemical Engineering 11 (2023) 109332

Contents lists available at ScienceDirect

Journal of Environmental Chemical Engineering

journal homepage: www.elsevier.com/locate/jece

Comparing the efficiency of solar water treatment: Photovoltaic-LED vs compound parabolic collector photoreactors

Miguel Martín-Sómer, María Dolores Molina-Ramírez, Maria Luisa Perez-Araujo, Rafael van Grieken, Javier Marugán *

Department of Chemical and Environmental Technology, ESCET, Universidad Rey Juan Carlos, C/ Tulipán s/n, 28933 Móstoles, Madrid, Spain

ARTICLE INFO

Editor: Despo Kassinos

Keywords:
Bacterial inactivation
Chemical pollutant oxidation
Solar CPC photoreactor
Solar PV panel
UVA LED
UVC LED

ABSTRACT

This work analyses how to optimise efficiency in the use of solar light for different UV-based photochemical water treatment processes. The direct use of sunlight in state-of-the-art compound parabolic collector (CPC) photoreactors is compared with the use of solar energy for electricity generation in photovoltaic (PV) power systems to feed LED lighting sources. Seven different solar processes (CPC, PV-UVA LED, PV-UVC LED, CPC+TiO_2, CPC+H_2O_2, PV-UVA LED+TiO_2 and PV–UVC LED+H_2O_2) were investigated, both for the oxidation of chemicals and the inactivation of bacteria. The results showed that, for the oxidation of chemicals, the best photochemical yield (in terms of the use of photons) is achieved by the PV-UVC LED+H_2O_2 process. However, the low electrical efficiency of current UVC LED sources makes the CPC+TiO_2 process the most efficient in the use of solar light. In contrast, for bacterial inactivation, the significantly higher effectiveness of the UVC spectral range in damaging DNA makes the PV-UVC LED+H_2O_2 the most efficient in the use of sunlight. When costs are considered, the PV-UVA LED+TiO_2 may be the most efficient process for chemical oxidation, while the PV-UVC LED+H_2O_2 process could be the most efficient for bacterial inactivation. These findings highlight the need to evaluate the optimal approach in reactor engineering for applications in the water-energy nexus, since the most efficient process for the use of solar light strongly depends on the electrical efficiency of the available PV and LED technology, which can be expected to be largely improved in the near future.

1. Introduction

For decades, radiation has been used in water treatment, allowing the inactivation of microorganisms [1–3] and the removal of chemical pollutants [4,5]. One of the key aspects to ensure the success of the process is the wavelength range of the employed radiation [6], with the use of UV light being necessary in most cases. The UV spectral range can be subdivided into UVC (100–280 nm), UVB (280–310 nm) and UVA (310–400 nm). The efficiency of UVC light in the inactivation of microorganisms, by alterations to their DNA chains, has been widely demonstrated [7,8]. The efficiency of UVA light is too low for this purpose [9], with UVB being intermediate [10]. In the case of chemical pollutants, for most compounds the single use of radiation does not produce significant degradation, being only photolysed those with a remarkable absorption. [11–13].

High-efficiency processes have been developed by incorporating photochemical processes and other agents in the so-called photo-activated advanced oxidation processes. These processes are mainly based on the generation of hydroxyl radicals which, through their high oxidising power, can remove a wide range of pollutants present in water, either chemical or microbiological nature [14–17].

Among the advanced photo-activated oxidation processes, it is worth mentioning the photo-Fenton process, which produces the decomposition of H_2O_2 through the use of ferrous salts as a catalyst, using light in the UVA-Visible range [18,19]. The UV/H_2O_2 process involves the formation of hydroxyl radicals by the photolysis of H_2O_2, requiring the use of light with a wavelength shorter than 300 nm [20,21]. Heterogeneous photocatalysis has been widely explored with TiO_2, or other semiconductor materials, which, after irradiation in the UVA range, are capable of producing hydroxyl radicals from water [22–24].

However, one of the major drawbacks of all the processes described above, and the main reason for their hindered industrial development is their high cost, due to the source of radiation [25]. In recent years, the development of the LED industry has produced a great expansion of UVA

* Corresponding author.
E-mail address: javier.marugan@urjc.es (J. Marugán).

https://doi.org/10.1016/j.jece.2023.109332
Received 2 December 2022; Received in revised form 4 January 2023; Accepted 14 January 2023
Available online 16 January 2023

LED and a similar evolution is expected for UVC LED in the forthcoming years [26].

An alternative for driving photochemical processes is the direct use of solar radiation, since around 6–7% of the light that reaches the earth's surface is within the UV range (mostly UVA and a small contribution of UVB) [27]. To improve the efficiency of the process, it is common to use compound parabolic collectors (CPC) to concentrate the light [28].

Despite the apparent environmental advantage of using direct sunlight to drive the process, the availability of low-cost solar photovoltaic panels (PV) for feeding LED systems increases the interest in alternative solar-powered photochemical water treatment processes due to cost reductions. However, despite the large amount of research available in the literature about the use of solar water treatment processes and LED photoreactors, since the early work of Bolton et al. on electrical and solar efficiency of AOP technologies [29], to the best of our knowledge, no studies have yet been conducted to compare the global energy efficiency in the use of solar light in both approaches. This work presents a comparative study of solar driven photo-activated water treatment processes based on the use of three different lighting sources: direct solar light in a CPC photoreactor; UVA LED and UVC LED (both of which are powered by a PV system) photoreactors. Seven different processes involving the potential presence of H_2O_2 and TiO_2 were tested and the efficiency of two test reactions were analysed: oxidation of methanol and inactivation of *E. coli* bacteria, as representatives of water decontamination and disinfection, respectively.

2. Material and methods

2.1. Photoreactors setup

A solar CPC photoreactor was used for experiments using direct solar light. It consisted of a borosilicate tube 26 mm in inner diameter and 380 mm in length (0.2 L of illuminated volume) located in the optical axis of a CPC aluminium reflector with 358 cm^2 of collection surface area that provides 85% light reflection towards the central pipe. The reactor operates in a closed recirculating circuit with a 1 L reservoir tank of water, driven by a centrifugal pump at a flow rate of 12 L/min [30].

For experiments based on LED light sources, an annular photoreactor (15 cm long, 3 cm internal diameter and 5 cm external diameter) was used, operating in a closed recirculation circuit with a 1 L reservoir tank, the water being driven by a centrifugal pump with a flow rate of 36 L/min. A schematic representation of the installation is given in [25]. As an illumination source, two different 8-LED based systems were used. For the experiments carried out with UVA light, LED with a maximum emission peak centred at 365 nm (LedEngin Model LZ1–00UV00) were used, while for the experiments with UVC light, LED with a maximum emission peak centred at 270 nm (Sum Tang ST-POBA20) were used (Fig. 1). The LED systems were continuously refrigerated using a liquid cooling system (Koolance EX2–755). The LED irradiation power was controlled by the electrical current intensity using the Eldoled LED driver Toolbox configuration software. In each case, the total irradiation power was calculated by potassium ferrioxalate actinometry experiments. In brief, a ferrioxalate solution is exposed to radiation, being reduced Fe^{3+} to Fe^{2+}. The formation of Fe^{2+} along the reaction is analysed by colourimetric quantification after forming a yellow compound by the addition of 1,10-phenanthroline. Known the quantum yield for the used wavelength, the incident radiation is then calculated from the reaction rate. Further details can be found elsewhere [31].

To power the LED system, an ATERSA GS 160 W Solar PV panel was used, with an output voltage of 12 V and a collection area of 1 m^2. The configuration of the LED connections (serial or parallel) was made in such a way that the total voltage was close to 12 V, to avoid the installation of a current inverter and the consequent loss of efficiency. The PV power system was connected to a Thlevel 30 A controller, coupled to a Ketotek voltmeter to quantify the energy produced. The LED system was connected to an Eleksol Lead-Acid 110Ah battery, as an alternative energy source. Although the LED system of the reactor could be operated without a battery during the day, the use of the supplementary power provides stability in the electrical supply. A schematic representation of the installation used is shown in Fig. 2.

The experiments were carried out at Universidad Rey Juan Carlos facilities in Móstoles, Spain (40.33° N, 3.86° W). Both the Solar CPC reflector and the Solar PV panel were placed with an inclination angle corresponding to the local latitude, as usually recommended for the

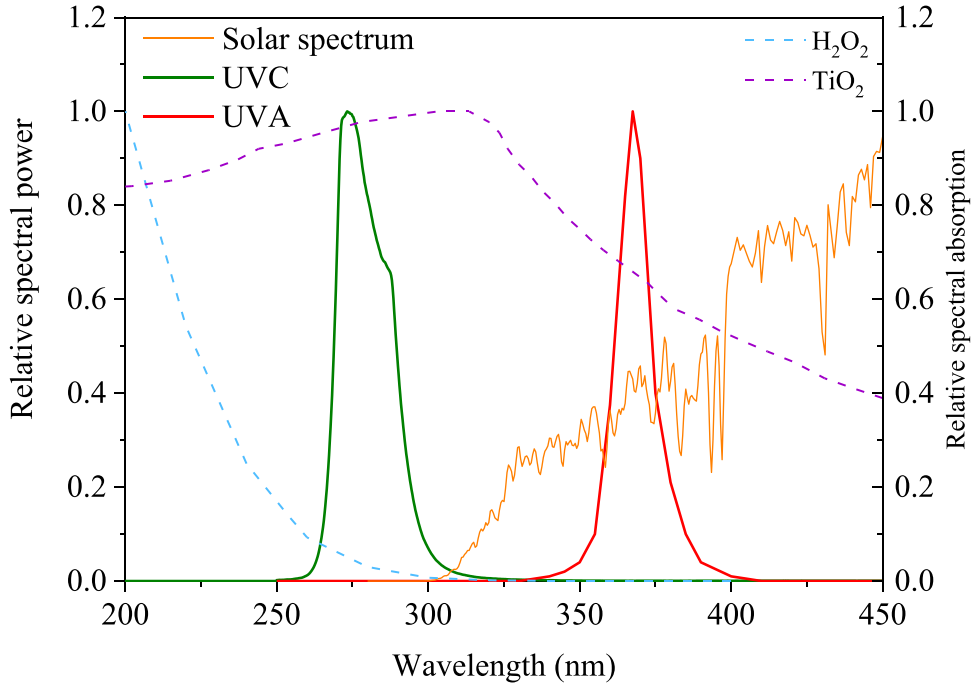

Fig. 1. Relative spectral power of UVC and UVA LED measured by an StellarNet UVIS-25 spectrometer, standard AM 1.5 solar spectrum [32] and relative spectral absorption of TiO_2 and H_2O_2 [33,34].

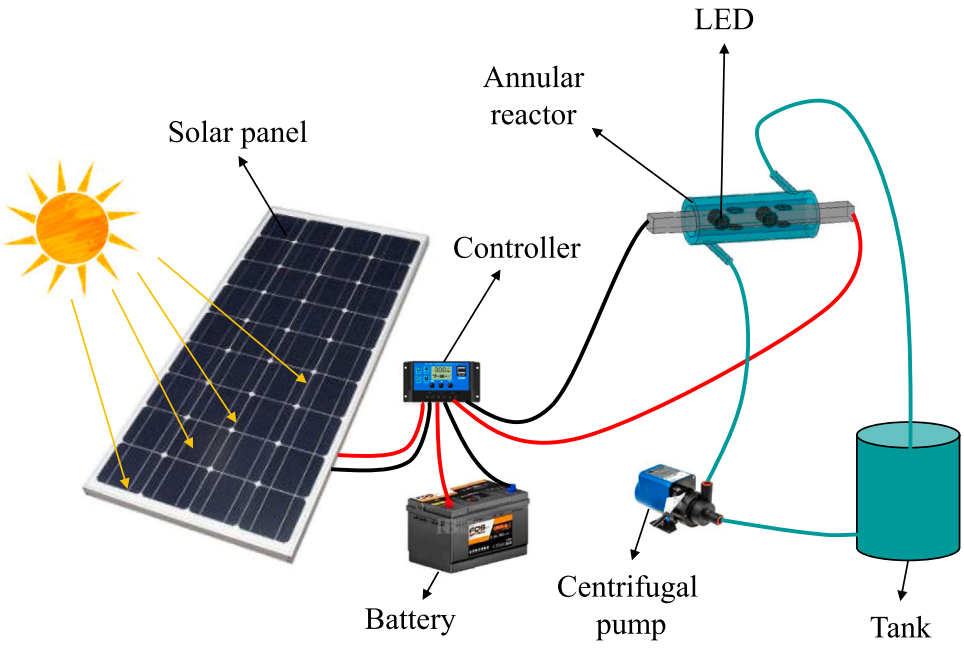

Fig. 2. Schematic representation of the LED reactor setup.

optimal operation of solar systems [35]. The solar irradiance was measured using a PCE-UV34 radiometer (290–390 nm). Temperature was monitored, not exceeding 30 ºC in any experiment.

2.2. Test reactions

For the comparison of the different treatments, two different test reactions were used. Methanol (Sigma-Aldrich, LC-MS), widely used as hydroxyl radical scavenger [36,37], was used as an indicator of the efficiency in the oxidation of chemical pollutants. Its organic nature turns methanol into a model compound to quantify the potential activity of an Advanced Oxidation Process (AOP). Moreover, oxidation of methanol to formaldehyde by direct photolysis is negligible, so the yield can be exclusively attributed to the photoactivated AOP. The initial concentration was fixed at 100 mM and all solutions were prepared in deionised water. The oxidation of methanol was followed through the colourimetric determination of the formaldehyde produced throughout the reaction [38], the quantitative oxidation product when methanol is in excess [36]. On the other hand, *E. coli* K12 strain (CECT 4624, corresponding to ATCC 23631, where CECT stands for 'Colección Española de Cultivos Tipo') was used as bacterial indicator for water disinfection experiments. Fresh liquid cultures were prepared by inoculation in a Luria-Bertani (LB) nutrient medium (Miller's LB Broth, Scharlab) and incubation during 24 h at 37 °C under constant stirring on a rotary shaker. The analysis of the samples was carried out throughout the reactions following a standard serial dilution procedure. Each decimal dilution was spotted on LB nutrient agar plates and incubated at 37 °C for 24 h before counting. To ensure the statistical significance of the results, a minimum of four replicates were carried out for all the experiments. The results were analysed based on the average of the replicates, using the standard deviation as a measurement of the experimental error.

Experiments with H_2O_2 were carried out using an initial concentration of 50 mg/L [39], ensuring a negligible depletion by using TP01000PX (Scharlab) indicator strips. Sodium sulphite (Na_2SO_3) was added in a Na_2SO_3-to-H_2O_2 molar ratio of 1:1 [40] after sample collection, to stop the oxidative action of H_2O_2. The experiments with H_2O_2 were not carried out in UVA radiation due to the need for a wavelength below 300 nm, to cause the H_2O_2 decomposition [20,21,41].

Photocatalytic processes were studied using Evonik P25 titanium dioxide suspensions at a concentration of 0.1 g/L, previously optimised [25].

Dark experiments were carried out both with TiO_2 and H_2O_2 to check if there was any interaction of these compounds in addition to the pure photocatalytic process for any of the pollutants studied.

3. Results

3.1. Photoelectrical characterisation

Ferrioxalate actinometry experiments were carried out to quantify the amount of radiation emitted by the UVA and UVC LED sources, as a function of the electrical power. The results shown in Fig. 3 show the large difference in the efficiency of electricity conversion into radiation between both lighting systems, with the UVA system producing four orders of magnitude more photons than the UVC system, for similar electrical power consumption. On the other hand, in both cases, it was possible to observe how the emission of the LED is directly proportional to the current, as expected from previous studies [25].

For the solar CPC photoreactors, different actinometrical experiments under natural sunlight were carried out on different days, to ensure the correlation between UV photons incident to the reactor and the cumulative radiation measured by the radiometer (Fig. 4), independently of weather conditions or time of the day. As expected, a linear trend with a reasonable correlation was clearly observed for the different replicates. This relationship allowed the estimation, for the subsequent reactions. of the radiation reaching the inside tube from the incident radiation measured by the radiometer. The value obtained for this relationship was 0.72 $E \cdot m^2/kWh$.

Finally, the amount of electrical energy produced by the solar PV panel was also quantified as a function of the solar radiation measured in the UV radiometer. Again, measurements were made under different weather conditions (sunny, cloudy and partly cloudy days) and at different time of the day, with the aim of predicting the energy production of the photovoltaic solar under a wide range of operational conditions. Fig. 5 shows the representation of these measurements, from which a ratio of 2.5 ($W_{generated}$ /$W_{UVsolar}$) was achieved for the surface of the solar panel (1 m^2).

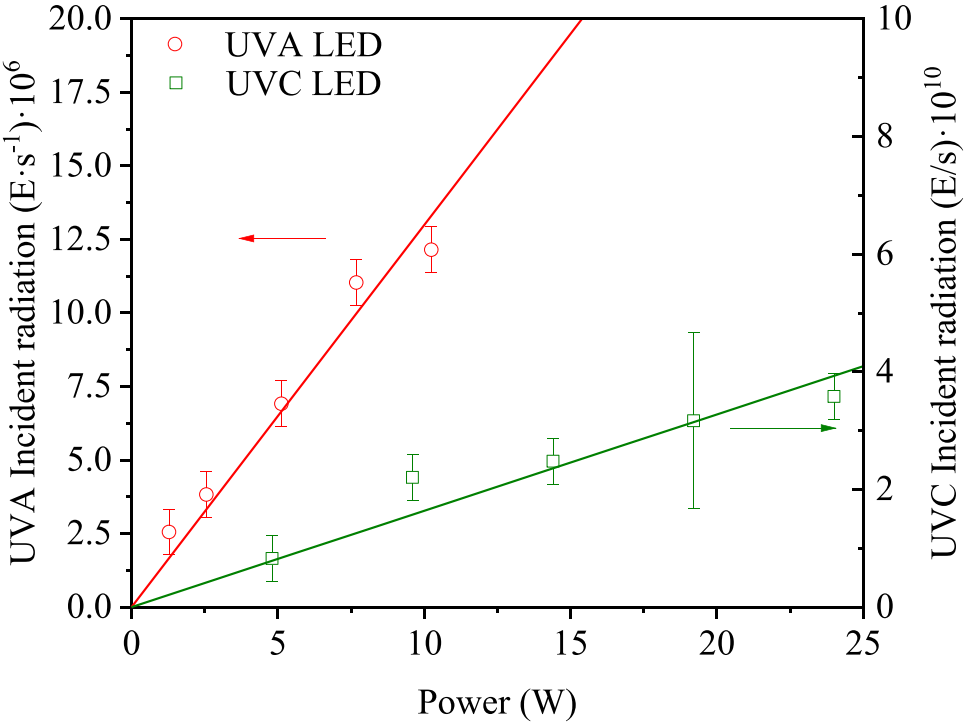

Fig. 3. Incident radiation measured by ferrioxalate actinometry for the UVC LED and UVA LED sources.

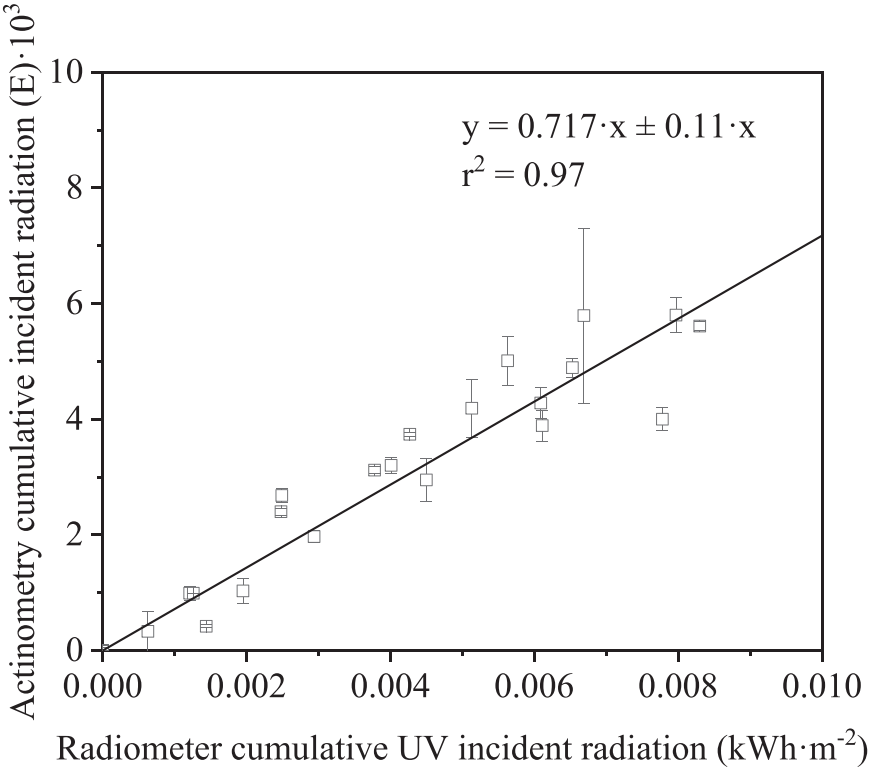

Fig. 4. Solar UV cumulative incident radiation measured by ferrioxalate actinometry in the CPC reactor versus cumulative incident radiation measured by a radiometer.

3.2. Oxidation of chemicals

Methanol oxidation experiments were carried out, the kinetic constant being calculated from the linear fit of the formaldehyde production data, as detailed elsewhere [25,30]. Fig. 6**a-e** shows the kinetic constants for the studied processes using different independent variables such as time, incident photons, power consumption and incident solar radiation.

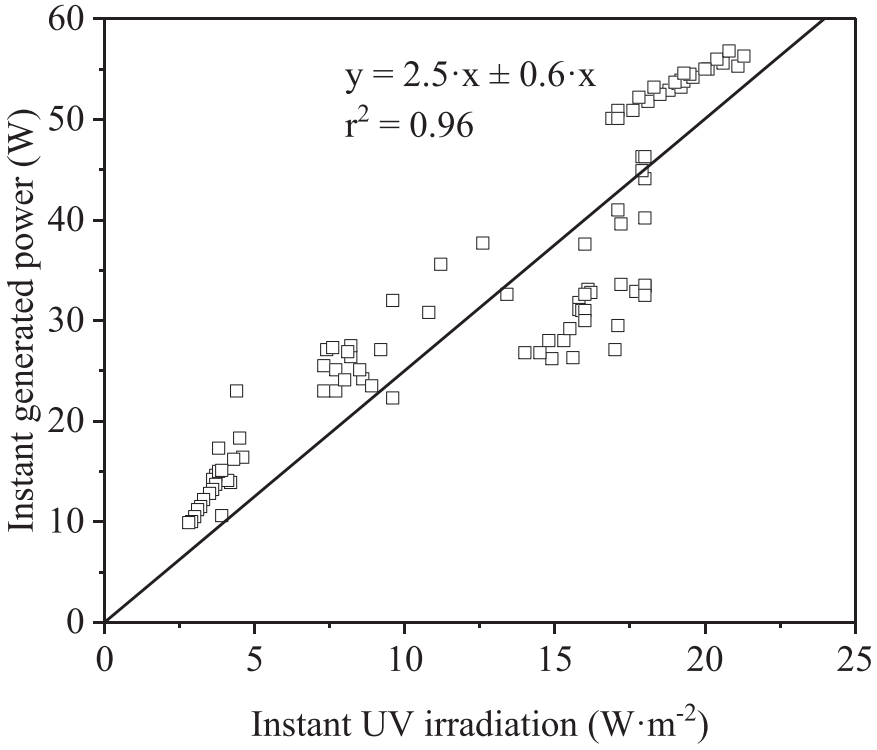

Fig. 5. Instant power generated by the solar PV panel as a function of the UV instant incident radiation measured in the radiometer.

Fig. 6**a** shows the kinetic constants obtained when formaldehyde concentration is plotted as a function of reaction time. Systems with higher oxidation rates are those based on the use of the TiO_2 catalyst, either using UVA LED or solar radiation. The process using UVC LED with H_2O_2 shows very little methanol removal, probably due to the low incident photon rate. For direct solar radiation, the kinetic constant obtained when using H_2O_2 is also low due to the low absorption coefficient of H_2O_2 at wavelengths above 300 nm [41]. In the case of using only light at any wavelength, the oxidation of methanol is almost nil, as expected by the negligible generation of oxidant species. It was also verified that in the absence of radiation, neither TiO_2 nor H_2O_2 does cause methanol oxidation.

Fig. 6**b** represents the kinetic constants obtained when considering the moles of formaldehyde as a function of the actual number of photons (E) that reached the reactor. In this case, UVC processes show a significantly higher efficiency in comparison with those based on UVA and direct sunlight. The efficiency of the UVC+H_2O_2 process is particularly remarkable, three orders of magnitude higher than that of the TiO_2 based photocatalytic process. On the other hand, if values obtained for the UVA LED and solar radiation are compared, it can be clearly seen that solar UV photons were used to a greater extent than those emitted by the LED source. In a previous work [30], it was verified that the degradation of methanol using TiO_2 at a specific wavelength was directly proportional to the absorption spectrum of TiO_2. The specific absorption coefficient of TiO_2, averaged according to the solar spectrum ASTM1.5 [32], could be obtained. Weighted calculations of the absorption of TiO_2 were carried out, taking into account the absorption spectrum (Fig. S1) and the solar irradiance for each wavelength (Fig. 1). Wavelengths up to 450 nm were considered, according to the light absorption in the actinometric ferrioxalate experiments [42]. The obtained value for the average specific absorption coefficient of the sunlight was 6234 cm^2/g whereas, for 365 nm, UVA LED was 8239 cm^2/g [30]. According to these values, a higher kinetic constant would be expected for the LED UVA process, which is the opposite of the experimental observations. However, another aspect to be considered is the influence of the light distribution on the efficiency of photocatalytic processes, due to the existence of recombination phenomena of electron-hole pairs in highly illuminated regions when light distribution is not uniform [25]. Radiation uniformity indices were obtained for both reactors, following the procedure published elsewhere [25]. In brief, the incident radiation field inside the reactor was modelled using Ansys Fluent 14.5 software and the uniformity index was calculated based on its distribution. This index represents how the values of a variable are distributed, a value of 1 being the highest uniformity, with a homogeneous value [43].

Uniformity index values of 0.38 and 0.81 were obtained for the UVA LED system and the solar CPC collector, respectively. Previous research has shown how the efficiency of the photocatalytic process is proportional to this uniformity parameter [25]. Therefore, this difference in uniformity between both systems overcomes the opposite trend mentioned for absorption coefficients, and it would explain the better photonic efficiency obtained in the CPC system.

Fig. 6**c** shows the kinetic constants obtained for LED-based systems when the electrical consumption is selected as an independent variable. In this case, the UVA+TiO_2 process is much more efficient than the UVC+H_2O_2 process. The reason for this is that the unquestionably higher photochemical efficiency of UVC photons shown in Fig. 6**b** is counteracted by the very low efficiency in the conversion of electricity into UVC radiation of current UVC LED sources.

On the other hand, Fig. 6**d** shows the kinetic constant obtained when formaldehyde concentration is plotted against the solar UV power, coming from the direct use of solar radiation collected in a CPC reactor (Eq. 1), or the use of solar radiation in the PV power system to produce electrical energy for the UV LED reactor (Eq. 2):

$$k\left(\frac{mol/L}{kWh_{UVsolar}}\right) = CPC_{eff}\left(\frac{E}{kWh_{UVsolar}/m^2\ x\ Area\ CPC\ (m^2)}\right) x\ k\left(\frac{mol/L}{E}\right) \quad (1)$$

where CPC_{eff} is the CPC concentration efficiency extracted from Fig. 4 and k is the kinetic constant referring to photons reaching the CPC photoreactor shown in Fig. 6**b**.

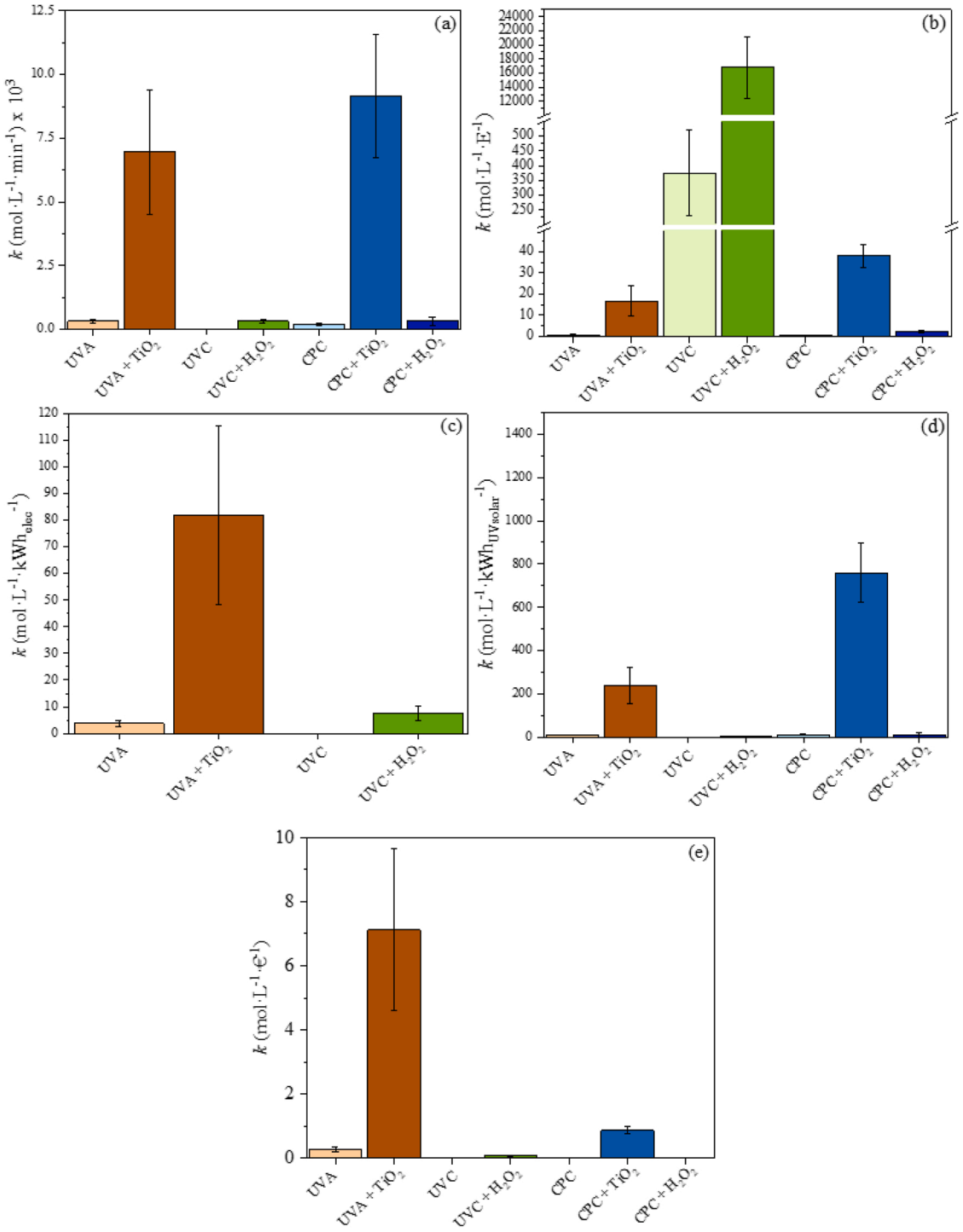

Fig. 6. Zero-order kinetic constant for methanol oxidation by the studied solar driven photochemical processes calculated as a function of (a) time (b) photons (c) energy consumption (d) solar UV radiation and (e) cost.

$$k\left(\frac{mol/L}{kWh_{UVsolar}}\right) = PV_{eff}\left(\frac{kW_{electric}}{kW_{UVsolar}/m^2\ x\ AreaPV\ (m^2)}\right) x\ LED_{eff}\left(\frac{E/h}{kW_{electric}}\right) x\ k\left(\frac{mol/L}{E}\right) \quad (2)$$

where PV_{eff} is the solar panel efficiency calculated in Fig. 5, LED_{eff} is the LED efficiency obtained from actinometry experiments. and k is the kinetic constant referring to photons reaching the photoreactor shown in Fig. 6**b**.

Regarding efficiency in the use of solar light, the UV energy harvested by each system is based on its collection surface (0.0358 m^2 for

the CPC and 1 m^2 for the solar PV panel). The results show that, despite the significant increase in the efficiency of UV LED and PV panels in recent years, the use of direct sunlight in a CPC photoreactor is still more efficient.

Another important aspect that must be evaluated when choosing a technology is the cost. In the specific case of the research carried out in this work, the price obtained by adding the different parts purchased for the assembly of the PV+UV LED systems (including solar panel, battery, UV LED, inverter, controller and annular reactor) was 435 € and 377.8 € for PV+UVA LED and PV+UVC LED, respectively, while the estimated price of the solar collector extracted from a previous work was 417 € [28]. For the calculation of the price of both systems, common elements such as centrifugal pumps and pipes were excluded. Taking these prices into account, new constants were calculated to reflect the installation cost following Eqs. 3 and 4. This constant was calculated using a reference solar radiation (RR) of 30 W/m^2 and a reference time (RT) of 1 h.

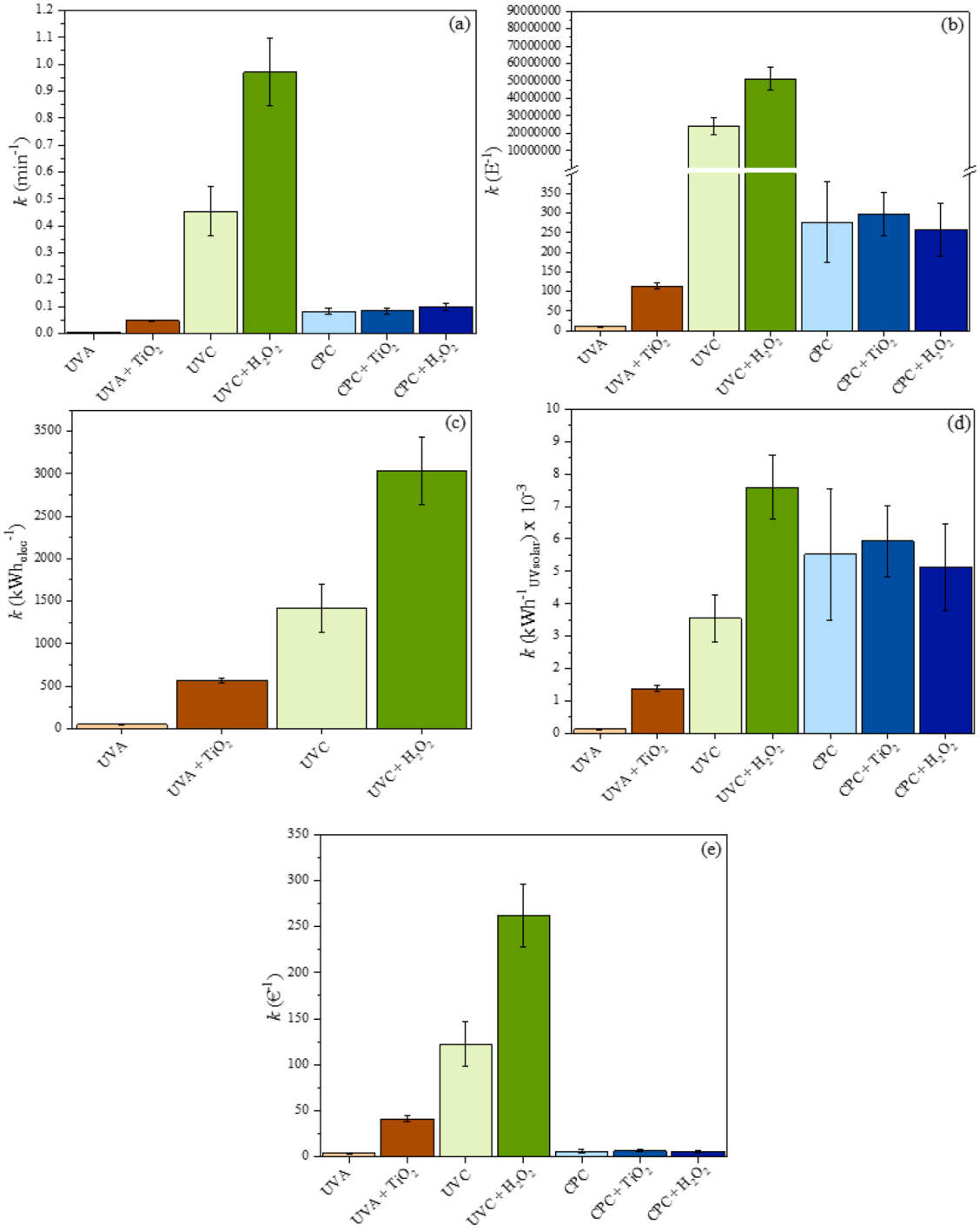

Fig. 7. First-order kinetic constant for bacterial inactivation in different processes obtained as a function of (a) time (b) photons (c) energy consumption (d) solar UV radiation and (e) cost.

$$k\left(\frac{mol/L}{€}\right) = CPC_{eff}\left(\frac{E}{kWh_{UVsolar}\ /\ m^2\ \text{x}\ AreaCPC\ (m^2)\ x\ PVCost\ \left(\frac{€}{m^2}\right)}\right) x\ RR\left(\frac{kW}{m^2}\right)\ \text{x}\ RT\ (h)\ \text{x}\ k\left(\frac{mol/L}{E}\right) \quad (3)$$

$$k\left(\frac{mol/L}{€}\right) = PV_{eff}\left(\frac{kW_{electric}}{kW_{UVsolar}\ /\ m^2\ x\ Area\ PV\ (m^2)\ x\ PV\ Cost\ \left(\frac{€}{m^2}\right)}\right) x\ LED_{eff}\left(\frac{E\ /\ h}{kW_{electric}}\right)\ \text{x}\ RR\left(\frac{kW}{m^2}\right) x\ RT\ (h)\ x\ k\left(\frac{mol\ /\ L}{E}\right) \quad (4)$$

Cost-based results are shown in Fig. 6**e**, the most economic option for carrying out the oxidation process being the PV-UVA LED system with TiO_2. It is worth noting that the costs cannot be extrapolated and may vary significantly over time and in different markets. Therefore, this conclusion should not be taken as absolute and calculations on current costs for every specific application should be conducted. In any case, it is important to note that the development of both LED and photovoltaic technology towards more efficient systems seems to indicate that the use of joint PV+LED systems will be the most efficient in this type of process in the near future. This conclusion applies not only to the studied processes, but it can be reasonably extrapolated to other technologies such as UV/Cl_2 or sulphate radical based photoactivated processes.

3.3. Bacterial inactivation

$$Solar_{eff\_LED}\left(\frac{1}{kWh_{UVsolar}}\right) = PV_{eff}\left(\frac{kW_{electric}}{kW_{UVsolar}\ /\ m^2\ x\ Area\ PV\ (m^2)}\right) x\ LED_{eff}\left(\frac{E/h}{kW_{electric}}\right) x\ k\left(\frac{1}{E}\right) \quad (6)$$

Experiments similar to those carried out for methanol oxidation were performed for bacterial inactivation. Kinetic constants were obtained for each type of reaction, fitting the results to a first order kinetics to obtain comparable parameters.

Fig. 7**a** shows the kinetic constants for bacterial inactivation obtained as a function of reaction time. Contrary to the oxidation of methanol, bacterial inactivation is significantly faster with UVC processes, especially the UVC+H_2O_2 combination. UVA light alone is not capable of causing any significant damage to bacteria and the remaining processes have similar efficiencies. It is remarkable that there are no significant differences between the use of direct sunlight in the CPC reactor and the use of sunlight combined with TiO_2 or H_2O_2. The use of sunlight alone is capable of inactivating bacteria due to the existence of part of the light in the UVB range. However, the use of TiO_2 does not produce a synergistic effect because most of the light is absorbed by the catalyst, preventing inactivation. In the case of adding H_2O_2, due to the minimal presence of light below 300 nm, its decomposition is scarce and, therefore, its effect is negligible. Bacterial inactivation was not observed in the presence of H_2O_2 alone.

Fig. 7**b** represents the kinetic constants obtained when considering the moles of photons (E) reaching the reactors. In this case, considering that the actual number of photons of UVC LED sources is much lower than photons generated in the other processes, the photochemical efficiencies are five orders of magnitude higher, as expected from the selective DNA damaging mechanism. On the other hand, it was possible to verify how direct solar processes are much more efficient than UVA LED-based processes due to the remarkable effect of the UVB fraction of solar light [10,44,45].

When referring to the electrical energy consumption, behaviour opposite to that previously described for methanol oxidation can be observed in Fig. 7**c**. Due to the great efficiency of UVC light in bacterial inactivation processes, and despite the poor electrical efficiency of UVC LED, the use of this type of radiation represented an energy improvement compared to the use of UVA LED.

On the other hand, solar energy efficiency for bacterial inactivation was obtained in a similar way as for methanol following the equations for CPC and LED systems:

$$Solar_{eff.CPC}\left(\frac{1}{kWh_{UVsolar}}\right) = CPC_{eff}\left(\frac{E}{kWh_{UVsolar}\ /\ m^2\ x Area CPC(m^2)}\right) xk\left(\frac{1}{E}\right) \quad (5)$$

The results (Fig. 7**d**) showed that the use of the UVC LED+H_2O_2, powered by a PV system, allowed a better use of solar radiation than the processes carried out in the CPC reactor. The sole use of UVC LED showed slightly worse results than the sole use of sunlight in the CPC reactor. However, it is necessary to consider that the electrical efficiency of UVC LED is increasing exponentially, so this result could be reversed very soon. During the development period of this study, the manufacturer reported that the efficiency of the UVC LED used had already increased its maximum from 72 to 112 mw. If these new LED were now used, the efficiency obtained with the use of UVC light alone would be $5.5{\cdot}10^3$ $kWh^{-1}_{UVsolar}$, already reaching the efficiency of CPC with direct sunlight.

On the other hand, the use of UVA LED for bacterial inactivation does not show these improvements and as seen in methanol oxidation, the use of direct solar light is more efficient.

If the efficiency is calculated considering the cost according to Eqs. 7 and 8, the results show an even more remarkable advantage of PV-UVC LED both with and without H_2O_2 (Fig. 7**e**). Additionally, considering the costs, the use of PV-UVA LED with TiO_2 is now more profitable than the use of direct sunlight. These results highlight that the use of combined systems with PV+UV LED should already be considered when designing solar water disinfection systems.

To facilitate the analysis of the results shown throughout this section, all the kinetic constants are summarised in Tables 1 and 2.

$$Solar_{eff}\left(\frac{1}{€}\right) = CPC_{eff}\left(\frac{E}{kWh_{UVsolar}/m^2}\right) x\ RR\left(\frac{kW}{m^2}\right) x\ RT\ (h)\ x\ k\left(\frac{1}{E}\right) \quad (7)$$

Table 1
Zero-order kinetic constant for methanol oxidation in the studied processes as a function of time, photons, energy consumption, solar UV radiation and investment cost.

	Time k ($mol{\cdot}L^{-1}{\cdot}min^{-1}$)	Photons k ($mol{\cdot}L^{-1}{\cdot}E^{-1}$)	Energy consumption k ($mol{\cdot}L^{-1}{\cdot}kWh_{elec}^{-1}$)	Solar UV radiation k ($mol{\cdot}L^{-1}{\cdot}kWh_{UVsolar}^{-1}$)	Investment cost k ($mol{\cdot}L^{-1}{\cdot}€^{-1}$)
UVA	$(3.14 \pm 0.89){\cdot}10^{-4}$	$(7.58 \pm 2.15){\cdot}10^{-1}$	$(3.68 \pm 1.05){\cdot}10^{-3}$	$(9.21 \pm 2.61){\cdot}10^{0}$	$(2.76 \pm 0.78){\cdot}10^{-1}$
UVA + TiO_2	$(6.96 \pm 2.45){\cdot}10^{-3}$	$(1.68 \pm 0.69){\cdot}10^{1}$	$(8.16 \pm 3.35){\cdot}10^{-2}$	$(2.37 \pm 0.84){\cdot}10^{2}$	$(7.12 \pm 2.51){\cdot}10^{0}$
UVC	$(7.14 \pm 2.75){\cdot}10^{-6}$	$(3.76 \pm 1.45){\cdot}10^{2}$	$(2.23 \pm 0.45){\cdot}10^{-5}$	$(5.58 \pm 2.15){\cdot}10^{-2}$	$(1.93 \pm 0.74){\cdot}10^{-4}$
UVC + H_2O_2	$(3.20 \pm 0.82){\cdot}10^{-4}$	$(1.68 \pm 0.43){\cdot}10^{4}$	$(7.54 \pm 2.15){\cdot}10^{-3}$	$(2.50 \pm 0.64){\cdot}10^{0}$	$(8.61 \pm 2.22){\cdot}10^{-2}$
CPC	$(2.00 \pm 0.63){\cdot}10^{-4}$	$(5.85 \pm 1.70){\cdot}10^{-1}$	-	$(1.17 \pm 0.34){\cdot}10^{1}$	$(1.26 \pm 0.37){\cdot}10^{-2}$
CPC + TiO_2	$(9.15 \pm 2.41){\cdot}10^{-3}$	$(3.79 \pm 0.53){\cdot}10^{1}$	-	$(7.60 \pm 1.35){\cdot}10^{2}$	$(8.64 \pm 1.13){\cdot}10^{-1}$
CPC + H_2O_2	$(3.21 \pm 1.58){\cdot}10^{-4}$	$(2.26 \pm 0.61){\cdot}10^{0}$	-	$(9.69 \pm 9.85){\cdot}10^{0}$	$(8.90 \pm 3.29){\cdot}10^{-4}$

Table 2
First-order kinetic constant for bacterial inactivation in the studied processes as a function of time, photons, energy consumption, solar UV radiation and investment cost.

	Time k (min^{-1})	Photons k (E^{-1})	Energy consumption k (kWh_{elec}^{-1})	Solar UV radiation k ($kWh_{UVsolar}^{-1}$)	Investment cost k ($€^{-1}$)
UVA	$(4.20 \pm 4.24){\cdot}10^{-3}$	$(1.01 \pm 0.10){\cdot}10^{1}$	$(4.92 \pm 0.50){\cdot}10^{-2}$	$(1.23 \pm 0.12){\cdot}10^{2}$	$(3.69 \pm 0.37){\cdot}10^{0}$
UVA + TiO_2	$(4.71 \pm 0.35){\cdot}10^{-2}$	$(1.13 \pm 0.08){\cdot}10^{2}$	$(5.65 \pm 0.33){\cdot}10^{-1}$	$(1.38 \pm 0.10){\cdot}10^{3}$	$(4.13 \pm 0.31){\cdot}10^{1}$
UVC	$(4.53 \pm 0.91){\cdot}10^{-1}$	$(2.39 \pm 0.48){\cdot}10^{7}$	$(1.42 \pm 0.29){\cdot}10^{0}$	$(3.54 \pm 0.71){\cdot}10^{3}$	$(1.22 \pm 0.25){\cdot}10^{2}$
UVC + H_2O_2	$(9.70 \pm 0.13){\cdot}10^{-1}$	$(5.11 \pm 0.67){\cdot}10^{7}$	$(3.04 \pm 0.40){\cdot}10^{0}$	$(7.59 \pm 0.99){\cdot}10^{3}$	$(2.62 \pm 0.34){\cdot}10^{2}$
CPC	$(8.10 \pm 1.12){\cdot}10^{-2}$	$(2.77 \pm 1.02){\cdot}10^{2}$	-	$(5.52 \pm 2.04){\cdot}10^{3}$	$(5.93 \pm 2.19){\cdot}10^{0}$
CPC + TiO_2	$(8.31 \pm 1.18){\cdot}10^{-2}$	$(2.97 \pm 0.55){\cdot}10^{2}$	-	$(5.93 \pm 1.09){\cdot}10^{3}$	$(6.37 \pm 1.17){\cdot}10^{0}$
CPC + H_2O_2	$(9.81 \pm 1.14){\cdot}10^{-2}$	$(2.57 \pm 0.67){\cdot}10^{2}$	-	$(5.13 \pm 1.34){\cdot}10^{3}$	$(5.51 \pm 1.43){\cdot}10^{0}$

$$Solar_{eff}\left(\frac{1}{€}\right) = Panel_{eff}\left(\frac{KW_{electric}}{kW_{UVsolar} \,/\, m^2 \; x \; Area\; PV\; (m^2) \; x \; PV\; Cost\; \left(\frac{€}{m^2}\right)}\right) x\; LED_{eff}\left(\frac{E/h}{kW_{electric}}\right) x\; RR\left(\frac{kW}{m^2}\right) x\; RT\;(h)\; x\; k\left(\frac{1}{E}\right) \tag{8}$$

4. Conclusions

UVC photons have a higher photochemical efficiency than UVA and solar photons, both for the inactivation of bacteria and the oxidation of chemicals. However, the low electrical efficiency of current UVC LED sources leads to a limited global efficiency in the use of solar light by its integration with PV power systems. For the oxidation of chemicals, the CPC+TiO_2 process showed a higher efficiency, followed by the PV-UVA LED+TiO_2 system. The reason is that, in all cases, the underlying mechanism is essentially the same, based on the generation of unselective oxidising hydroxyl radicals. In contrast, for bacterial inactivation, the high selectivity of the DNA damaging UVC LED mechanism, compared to the rest of the processes, makes the PV-UVC LED+H_2O_2 process the most efficient alternative. These conclusions, based on the efficiency of currently available PV and UV LED technologies, will definitively make their case for future applications if their electrical efficiency (especially of UVC LED), increases as expected and their price in the market progressively decreases. In fact, if costs are considered for the systems used in this work, the use of PV-LED UVA + TiO_2 and PV-UVC LED+H_2O_2 are already the most cost-effective alternatives for chemical oxidation and bacterial inactivation, respectively. Although the conclusions of this work are obtained from specific systems and could slightly vary with other reactor designs of different light distribution, from a qualitative point of view they can be certainly extrapolated to the analysis of future application of solar water treatment processes.

CRediT authorship contribution statement

M. Martín-Sómer: Conceptualization, Methodology, Investigation, Data curation, Visualization, Writing – original draft. **M.D. Molina-Ramírez**: Investigation, Writing – review. **M.L. Pérez-Araujo**: Investigation, Writing – review. **R. van Grieken**: Supervision, Methodology, Writing – review & editing. **J. Marugán**: Supervision, Conceptualization, Methodology, Writing – review & editing, Funding acquisition.

Declaration of Competing Interest

The authors declare that they have no known competing financial interests or personal relationships that could have appeared to influence the work reported in this paper.

Data availability

Data will be made available on request.

Acknowledgements

The authors gratefully acknowledge the financial support of the European Union's Horizon 2020 research and innovation programme in the frame of the PANIWATER project (GA 820718), funded under the Indo-EU International Water Cooperation sponsored jointly by European Commission and Department of Science and Technology, India, and the Spanish State Research Agency (AEI) and the Spanish Ministry of Science and Innovation through the project AQUAENAGRI (PID2021-126400OB-C32).

Appendix A. Supporting information

Supplementary data associated with this article can be found in the online version at doi:10.1016/j.jece.2023.109332.

References

[1] J. Foschi, A. Turolla, M. Antonelli, Artificial neural network modeling of full-scale UV disinfection for process control aimed at wastewater reuse, J. Environ. Manag. 300 (2021), 113790, https://doi.org/10.1016/J.JENVMAN.2021.113790.

[2] Z. Sun, M. Li, W. Li, Z. Qiang, A review of the fluence determination methods for UV reactors: ensuring the reliability of UV disinfection, Chemosphere 286 (2022), 131488, https://doi.org/10.1016/J.CHEMOSPHERE.2021.131488.

[3] Q. Zhao, N. Li, C. Liao, L. Tian, J. An, X. Wang, The UV/H2O2 process based on H2O2 in-situ generation for water disinfection, J. Hazard. Mater. Lett. 2 (2021), 100020, https://doi.org/10.1016/J.HAZL.2021.100020.

[4] J. Wang, J. Zhang, S.Q. Huang, Y. Hu, Y. Mu, Treatment of iodine-containing water by the UV/NH2Cl process: dissolved organic matters transformation, iodinated trihalomethane formation and toxicity variation, Water Res. 200 (2021), 117256, https://doi.org/10.1016/J.WATRES.2021.117256.

[5] C.W. Pai, G.S. Wang, Treatment of PPCPs and disinfection by-product formation in drinking water through advanced oxidation processes: comparison of UV, UV/Chlorine, and UV/H2O2, Chemosphere 287 (2022), 132171, https://doi.org/10.1016/J.CHEMOSPHERE.2021.132171.

[6] J. Wang, H. Liu, Y. Wang, D. Ma, G. Yao, Q. Yue, B. Gao, X. Xu, A new UV source activates ozone for water treatment: wavelength-dependent ultraviolet light-emitting diode (UV-LED, Sep. Purif. Technol. 280 (2022), 119934, https://doi.org/10.1016/J.SEPPUR.2021.119934.

[7] V. Baldasso, H. Lubarsky, N. Pichel, A. Turolla, M. Antonelli, M. Hincapie, L. Botero, F. Reygadas, A. Galdos-Balzategui, J.A. Byrne, P. Fernandez-Ibañez, UVC inactivation of MS2-phage in drinking water – modelling and field testing, Water Res. 203 (2021), 117496, https://doi.org/10.1016/J.WATRES.2021.117496.

[8] C.P. Wang, C.S. Chang, W.C. Lin, Efficiency improvement of a flow-through water disinfection reactor using UV-C light emitting diodes, J. Water Process Eng. 40 (2021), 101819, https://doi.org/10.1016/j.jwpe.2020.101819.

[9] K.G. McGuigan, R.M. Conroy, H.J. Mosler, M. du Preez, E. Ubomba-Jaswa, P. Fernandez-Ibañez, Solar water disinfection (SODIS): a review from bench-top to roof-top, J. Hazard. Mater. 235–236 (2012) 29–46, https://doi.org/10.1016/j.jhazmat.2012.07.053.

[10] H.D. Minh Tran, S. Boivin, H. Kodamatani, K. Ikehata, T. Fujioka, Potential of UV-B and UV-C irradiation in disinfecting microorganisms and removing N-nitrosodimethylamine and 1,4-dioxane for potable water reuse: a review, Chemosphere 286 (2022), 131682, https://doi.org/10.1016/J.CHEMOSPHERE.2021.131682.

[11] Y. Zhang, H. Wang, Y. Li, B. Wang, J. Huang, S. Deng, G. Yu, Y. Wang, Removal of micropollutants by an electrochemically driven UV/chlorine process for decentralized water treatment, Water Res. 183 (2020), 116115, https://doi.org/10.1016/J.WATRES.2020.116115.

[12] H. Ding, J. Hu, Degradation of carbamazepine by UVA/WO3/hypochlorite process: kinetic modelling, water matrix effects, and density functional theory calculations, Environ. Res. 201 (2021), 111569, https://doi.org/10.1016/J.ENVRES.2021.111569.

[13] S. Madihi-Bidgoli, S. Asadnezhad, A. Yaghoot-Nezhad, A. Hassani, Azurobine degradation using Fe2O3@multi-walled carbon nanotube activated peroxymonosulfate (PMS) under UVA-LED irradiation: performance, mechanism and environmental application, J. Environ. Chem. Eng. 9 (2021), 106660, https://doi.org/10.1016/J.JECE.2021.106660.

[14] M.Y. Kilic, W.H. Abdelraheem, X. He, K. Kestioglu, D.D. Dionysiou, Photochemical treatment of tyrosol, a model phenolic compound present in olive mill wastewater, by hydroxyl and sulfate radical-based advanced oxidation processes (AOPs), J. Hazard. Mater. 367 (2019) 734–742, https://doi.org/10.1016/J.JHAZMAT.2018.06.062.

[15] S. Barisci, R. Suri, Removal of polyfluorinated telomer alcohol by Advanced Oxidation Processes (AOPs) in different water matrices and evaluation of degradation mechanisms, J. Water Process Eng. 39 (2021), 101745, https://doi.org/10.1016/J.JWPE.2020.101745.

[16] M. Sgroi, S.A. Snyder, P. Roccaro, Comparison of AOPs at pilot scale: energy costs for micro-pollutants oxidation, disinfection by-products formation and pathogens inactivation, Chemosphere 273 (2021), 128527, https://doi.org/10.1016/J.CHEMOSPHERE.2020.128527.

[17] F.X. Tian, W.K. Ye, B. Xu, X.J. Hu, S.X. Ma, F. Lai, Y.Q. Gao, H.B. Xing, W.H. Xia, B. Wang, Comparison of UV-induced AOPs (UV/Cl2, UV/NH2Cl, UV/ClO2 and UV/H2O2) in the degradation of iopamidol: kinetics, energy requirements and DBPs-related toxicity in sequential disinfection processes, Chem. Eng. J. 398 (2020), 125570, https://doi.org/10.1016/J.CEJ.2020.125570.

[18] A.V. Vorontsov, Advancing Fenton and photo-Fenton water treatment through the catalyst design, J. Hazard. Mater. 372 (2019) 103–112, https://doi.org/10.1016/J.JHAZMAT.2018.04.033.

[19] N. Hassanshahi, A. Karimi-Jashni, Comparison of photo-Fenton, O3/H2O2/UV and photocatalytic processes for the treatment of gray water, Ecotoxicol. Environ. Saf. 161 (2018) 683–690, https://doi.org/10.1016/J.ECOENV.2018.06.039.

[20] C. Seo, J. Shin, M. Lee, W. Lee, H. Yoom, H. Son, S. Jang, Y. Lee, Elimination efficiency of organic UV filters during ozonation and UV/H2O2 treatment of drinking water and wastewater effluent, Chemosphere 230 (2019) 248–257, https://doi.org/10.1016/J.CHEMOSPHERE.2019.05.028.

[21] C.B. Alvim, V.R. Moreira, Y.A.R. Lebron, A.V. Santos, L.C. Lange, R.P.M. Moreira, L.V. de, S. Santos, M.C.S. Amaral, Comparison of UV, UV/H2O2 and ozonation processes for the treatment of membrane distillation concentrate from surface water treatment: PhACs removal and environmental and human health risk assessment, Chem. Eng. J. 397 (2020), 125482, https://doi.org/10.1016/J.CEJ.2020.125482.

[22] M.R. Al-Mamun, S. Kader, M.S. Islam, M.Z.H. Khan, Photocatalytic activity improvement and application of UV-TiO2 photocatalysis in textile wastewater treatment: a review, J. Environ. Chem. Eng. 7 (2019), 103248, https://doi.org/10.1016/J.JECE.2019.103248.

[23] S. Murgolo, C. De Ceglie, C. Di Iaconi, G. Mascolo, Novel TiO2-based catalysts employed in photocatalysis and photoelectrocatalysis for effective degradation of pharmaceuticals (PhACs) in water: a short review, Curr. Opin. Green Sustain. Chem. 30 (2021), 100473, https://doi.org/10.1016/J.COGSC.2021.100473.

[24] M.C. Dlamini, M.S. Maubane-Nkadimeng, J.A. Moma, The use of TiO2/clay heterostructures in the photocatalytic remediation of water containing organic pollutants: a review, J. Environ. Chem. Eng. 9 (2021), 106546, https://doi.org/10.1016/J.JECE.2021.106546.

[25] M. Martín-Sómer, C. Pablos, R. van Grieken, J. Marugán, Influence of light distribution on the performance of photocatalytic reactors: LED vs mercury lamps, Appl. Catal. B Environ. 215 (2017) 1–7, https://doi.org/10.1016/j.apcatb.2017.05.048.

[26] H. Amano, R. Collazo, C. De Santi, S. Einfeldt, M. Funato, J. Glaab, S. Hagedorn, A. Hirano, H. Hirayama, R. Ishii, Y. Kashima, Y. Kawakami, R. Kirste, M. Kneissl, R. Martin, F. Mehnke, M. Meneghini, A. Ougazzaden, P.J. Parbrook, S. Rajan, P. Reddy, F. Römer, J. Ruschel, B. Sarkar, F. Scholz, L.J. Schowalter, P. Shields, Z. Sitar, L. Sulmoni, T. Wang, T. Wernicke, M. Weyers, B. Witzigmann, Y.R. Wu, T. Wunderer, Y. Zhang, The 2020 UV emitter roadmap, J. Phys. D Appl. Phys. 53 (2020), 503001, https://doi.org/10.1088/1361-6463/ABA64C.

[27] S.M. Parsa, S. Momeni, A. Hemmat, M. Afrand, Effectiveness of solar water disinfection in the era of COVID-19 (SARS-CoV-2) pandemic for contaminated water/wastewater treatment considering UV effect and temperature, J. Water Process Eng. 43 (2021), 102224, https://doi.org/10.1016/J.JWPE.2021.102224.

[28] M. Martín-Sómer, J. Moreno-SanSegundo, C. Álvarez-Fernández, R. van Grieken, J. Marugán, High-performance low-cost solar collectors for water treatment fabricated with recycled materials, open-source hardware and 3d-printing technologies, Sci. Total Environ. 784 (2021) 147119. https://linkinghub.elsevier.com/retrieve/pii/S0048969721021896 (accessed April 21, 2021).

[29] J.R. Bolton, K.G. Bircher, W. Tumas, C.A. Tolman, Figures of merit for the technical development and application of advanced oxidation technologies for both electric- and solar-driven systems, Pure Appl. Chem. 73 (2001) 627–637, https://doi.org/10.1351/PAC200173040627/MACHINEREADABLECITATION/RIS.

[30] M. Martín-Sómer, B. Vega, C. Pablos, R. van Grieken, J. Marugán, Wavelength dependence of the efficiency of photocatalytic processes for water treatment, Appl. Catal. B Environ. 221 (2018) 258–265, https://doi.org/10.1016/J.APCATB.2017.09.032.

[31] C.G. Hatchard, C.A. Parker, A new sensitive chemical actinometer. II. Potassium ferrioxalate as a standard chemical actinometer, Proc. R. Soc. Lond. Ser. A Math. Phys. Sci. 235 (1956) 518 LP – 536. https://doi.org/10.1098/rspa.1956.0102.

[32] ASTM G173–03 Standard solar spectral irradiance AM 1.5, (n.d.).

[33] G. Kandregula, A. Chinthakuntla, K. Venkateswara Rao, V. Rajendar, K. Ganapathi Rao, C. Ashok, K. Venkateswara Rao, C. Shilpa Chakra, V. Rajendar, Green synthesis of TiO2 nanoparticles using hibiscus flower extract, 2014. https://www.researchgate.net/publication/303445315 (accessed November 29, 2022).

[34] Z. Liu, C. Zhou, D. Liu, T. He, L. Guo, D. Xu, M.G. Kong, Quantifying the concentration and penetration depth of long-lived RONS in plasma-activated water by UV absorption spectroscopy, AIP Adv. 9 (2019), 015014, https://doi.org/10.1063/1.5037660.

[35] S. Malato, P. Fernández-Ibáñez, M.I. Maldonado, J. Blanco, W. Gernjak, Decontamination and disinfection of water by solar photocatalysis: recent overview and trends, Catal. Today 147 (2009) 1–59, https://doi.org/10.1016/j.cattod.2009.06.018.

[36] L. Sun, J.R. Bolton, Determination of the quantum yield for the photochemical generation of hydroxyl radicals in TiO2 suspensions, J. Phys. Chem. 100 (1996) 4127–4134, https://doi.org/10.1021/jp9505800.

[37] C. Wang, D.W. Bahnemann, J.K. Dohrmann, Determination of photonic efficiency and quantum yield of formaldehyde formation in the presence of various TiO2 photocatalysts, Water Sci. Technol. 44 (2001) 279–286, https://doi.org/10.2166/WST.2001.0306.

[38] R.K. Eckert, H.W. Elliott, K.A.C. Elliott, K.A.C. Gustafson, F.G. Henderson, J. M. Bonner, J.; M.J. Jones, D.B. Kenten, R.H. Mann, P.J.G. Makino, K. Satoh, K. Fujiki, T. Kawaguchi, K. Stanier, R.Y. Tsuchida, M. Weil, L. Gordon, N.

G. Buchert, The colorimetric estimation of formaldehyde by means of the Hantzsch reaction, Biochem. J. 55 (1953) 416, https://doi.org/10.1042/BJ0550416.
[39] W.H. Chin, F.A. Roddick, J.L. Harris, Greywater treatment by UVC/H2O2, Water Res. 43 (2009) 3940–3947, https://doi.org/10.1016/J.WATRES.2009.06.050.
[40] W. Liu, S.A. Andrews, M.I. Stefan, J.R. Bolton, Optimal methods for quenching H2O2 residuals prior to UFC testing, Water Res. 37 (2003) 3697–3703, https://doi.org/10.1016/S0043-1354(03)00264-1.
[41] M.H.F. Graumans, W.F.L.M. Hoeben, F.G.M. Russel, P.T.J. Scheepers, Oxidative degradation of cyclophosphamide using thermal plasma activation and UV/H2O2 treatment in tap water, Environ. Res. 182 (2020), 109046, https://doi.org/10.1016/J.ENVRES.2019.109046.
[42] B. Wriedt, D. Ziegenbalg, Application limits of the ferrioxalate actinometer, ChemPhotoChem 5 (2021) 947–956, https://doi.org/10.1002/CPTC.202100122.
[43] ANSYS Fluent Theory Guide, 2013.
[44] E.G. Mbonimpa, B. Vadheim, E.R. Blatchley, Continuous-flow solar UVB disinfection reactor for drinking water, Water Res. 46 (2012) 2344–2354, https://doi.org/10.1016/J.WATRES.2012.02.003.
[45] M.B. Fisher, M. Iriarte, K.L. Nelson, Solar water disinfection (SODIS) of Escherichia coli, Enterococcus spp., and MS2 coliphage: effects of additives and alternative container materials, Water Res. 46 (2012) 1745–1754, https://doi.org/10.1016/J.WATRES.2011.12.048.